Rapidity and energy dependence of the electric charge correlations in $A+A$ collisions from 20A to 158A GeV

C. Alt,[9] T. Anticic,[23] B. Baatar,[8] D. Barna,[4] J. Bartke,[6] L. Betev,[10] H. Białkowska,[20] C. Blume,[9] B. Boimska,[20] M. Botje,[1] J. Bracinik,[3] R. Bramm,[9] P. Buncic,[10] V. Cerny,[3] P. Christakoglou,[2] P. Chung,[19] O. Chvala,[14] J. G. Cramer,[16] P. Csató,[4] P. Dinkelaker,[9] V. Eckardt,[13] D. Flierl,[9] Z. Fodor,[4] P. Foka,[7] V. Friese,[7] J. Gál,[4] M. Gaździcki,[9,11] V. Genchev,[18] G. Georgopoulos,[2] E. Gładysz,[6] K. Grebieszkow,[22] S. Hegyi,[4] C. Höhne,[7] K. Kadija,[23] A. Karev,[13] D. Kikola,[22] M. Kliemant,[9] S. Kniege,[9] V. I. Kolesnikov,[8] E. Kornas,[6] R. Korus,[11] M. Kowalski,[6] I. Kraus,[7] M. Kreps,[3] A. Laszlo,[4] R. Lacey,[19] M. van Leeuwen,[1] P. Lévai,[4] L. Litov,[17] B. Lungwitz,[9] M. Makariev,[17] A. I. Malakhov,[8] M. Mateev,[17] G. L. Melkumov,[8] A. Mischke,[1] M. Mitrovski,[9] J. Molnár,[4] St. Mrówczyński,[11] V. Nicolic,[23] G. Pálla,[4] A. D. Panagiotou,[2] D. Panayotov,[17] A. Petridis,[2] W. Peryt,[22] M. Pikna,[3] J. Pluta,[22] D. Prindle,[16] F. Pühlhofer,[12] R. Renfordt,[9] C. Roland,[5] G. Roland,[5] M. Rybczyński,[11] A. Rybicki,[6] A. Sandoval,[7] N. Schmitz,[13] T. Schuster,[9] P. Seyboth,[13] F. Siklér,[4] B. Sitar,[3] E. Skrzypczak,[21] M. Slodkowski,[22] G. Stefanek,[11] R. Stock,[9] C. Strabel,[9] H. Ströbele,[9] T. Susa,[23] I. Szentpétery,[4] J. Sziklai,[4] M. Szuba,[22] P. Szymanski,[10,20] V. Trubnikov,[20] D. Varga,[4,10] M. Vassiliou,[2] G. I. Veres,[4,5] G. Vesztergombi,[4] D. Vranić,[7] A. Wetzler,[9] Z. Włodarczyk,[11] A. Wojtaszek,[11] I. K. Yoo,[15] and J. Zimányi[4,*]

(NA49 Collaboration)

[1]*NIKHEF, Amsterdam, Netherlands*
[2]*Department of Physics, University of Athens, Athens, Greece*
[3]*Comenius University, Bratislava, Slovakia*
[4]*KFKI Research Institute for Particle and Nuclear Physics, Budapest, Hungary*
[5]*MIT, Cambridge, Massachusetts, USA*
[6]*Henryk Niewodniczanski Institute of Nuclear Physics, Polish Academy of Sciences, Cracow, Poland*
[7]*Gesellschaft für Schwerionenforschung (GSI), Darmstadt, Germany*
[8]*Joint Institute for Nuclear Research, Dubna, Russia*
[9]*Fachbereich Physik der Universität, Frankfurt, Germany*
[10]*CERN, Geneva, Switzerland*
[11]*Institute of Physics Świętokrzyska Academy, Kielce, Poland*
[12]*Fachbereich Physik der Universität, Marburg, Germany*
[13]*Max-Planck-Institut für Physik, Munich, Germany*
[14]*Charles University, Faculty of Mathematics and Physics, Institute of Particle and Nuclear Physics, Prague, Czech Republic*
[15]*Department of Physics, Pusan National University, Pusan, Republic of Korea*
[16]*Nuclear Physics Laboratory, University of Washington, Seattle, Washington, USA*
[17]*Atomic Physics Department, Sofia University, St. Kliment Ohridski, Sofia, Bulgaria*
[18]*Institute for Nuclear Research and Nuclear Energy, Sofia, Bulgaria*
[19]*Department of Chemistry, Stony Brook University (SUNYSB), Stony Brook, New York, USA*
[20]*Institute for Nuclear Studies, Warsaw, Poland*
[21]*Institute for Experimental Physics, University of Warsaw, Warsaw, Poland*
[22]*Faculty of Physics, Warsaw University of Technology, Warsaw, Poland*
[23]*Rudjer Boskovic Institute, Zagreb, Croatia*

(Received 16 April 2007; published 27 August 2007)

Results from electric charge correlations studied with the Balance Function (BF) method in $A+A$ collisions from 20A to 158A GeV are presented in two different rapidity intervals: In the midrapidity region we observe a decrease of the width of the BF distribution with increasing centrality of the collision, whereas this effect vanishes in the forward rapidity region. Results from the energy dependence study in central Pb+Pb collisions show that the narrowing of the BF expressed by the normalized width parameter W increases with energy toward the highest CERN Super Proton Synchrotron and BNL Relativistic Heavy Ion Collider energies. Finally we compare our experimental data points with the predictions of several models. The hadronic string models Ultra-relativistic Quantum Molecular Dynamics and Heavy Ion Jet INteraction Generator (HIJING) do not reproduce the observed narrowing of the BF. However, A MultiPhase Transport medel (AMPT), which contains a quark-parton transport phase before hadronization, can reproduce the narrowing of the BF's width with centrality. This confirms the proposed sensitivity of the BF analysis to the time of hadronization.

DOI: 10.1103/PhysRevC.76.024914 PACS number(s): 25.75.Gz

I. INTRODUCTION

The study of the Balance Function (BF) is motivated by the prediction that its width may be sensitive to the creation of a

[*]Deceased.

deconfined phase in the early stage of central nucleus-nucleus collisions [1–3]. The method is based on the observation that hadrons are produced locally in pairs of oppositely charged particles. Because of the initial momentum difference and secondary interactions with other particles, these particles are separated in rapidity (y). Particles of a pair that was created earlier are separated further in rapidity because of the expected large initial momentum difference and the long lasting rescattering phase. On the other hand, momentum differences of charged particles of a pair that was created later in the reaction are mainly determined by the breakup temperature. The previous two opposite mechanisms are reflected in the BF's width and result in a narrow distribution for the late stage hadronization scenario and a wide one for the early stage hadron production [1,4,5]. Our aim is to find a possible indication of a delayed hadronization.

It was suggested that the creation of a deconfined phase of quarks and gluons (the quark-gluon plasma, QGP) in the early stages of nucleus-nucleus collisions would lead to delayed hadronization, i.e. a narrowing of the BF [1]. Indeed, results on the BF obtained for Au+Au collisions at BNL Relativistic Heavy Ion Collider (RHIC) [5] and Pb+Pb interactions at the top CERN Super Proton Synchrotron (SPS) energy [4] show this narrowing for central collisions in the midrapidity domain. In this article, the study of the BF is extended to the forward rapidity region. In addition, the energy dependence of the width of the BF for central Pb+Pb collisions is investigated at lower SPS energies where indications for the onset of deconfinement have been obtained [6].

As in previous publications from the NA49 experiment on the BF [4], the analysis is performed for all charged particles (predominantly pions) to avoid the additional complications from the identification procedure. Consequently the pseudorapidity (η) of charged particles is examined and the BF is defined as [1]

$$B(\Delta\eta) = \frac{1}{2}\left[\frac{N_{+-}(\Delta\eta) - N_{--}(\Delta\eta)}{N_-} + \frac{N_{-+}(\Delta\eta) - N_{++}(\Delta\eta)}{N_+}\right]. \quad (1)$$

The width of the BF can be characterized by the weighted average $\langle\Delta\eta\rangle$,

$$\langle\Delta\eta\rangle = \sum_{i=0}^{k}(B_i \cdot \Delta\eta_i) \Big/ \sum_{i=0}^{k} B_i, \quad (2)$$

where i is the bin number of the BF histogram.

In the following two sections we first describe in brief the NA49 experimental setup and the data analysis. The next two sections are dedicated to the new experimental results on the rapidity and the energy dependence of the width of the BF. We conclude with a section on model comparisons and a summary.

II. EXPERIMENTAL SETUP

The NA49 detector [7] is a wide acceptance hadron spectrometer for the study of hadron production in collisions of hadrons or heavy ions at the CERN SPS. The main components are four large-volume Time Projection Chambers (TPCs) that are capable of detecting 80% of some 1500 charged particles created in a central Pb+Pb collision at 158A GeV.

The targets are C (561 mg/cm^2) and Si (1170 mg/cm^2) disks and a Pb (224 mg/cm^2) foil for ion collisions and a liquid hydrogen cylinder (length 20 cm) for hadron interactions. They are positioned about 80 cm upstream from VTPC-1.

The centrality of a collision is selected (on-line for central Pb+Pb, Si+Si, and C+C interactions and off-line for minimum bias Pb+Pb, Si+Si, and C+C interactions) by a trigger using information from a downstream calorimeter (VCAL), which measures the energy E_0 of the projectile spectator nucleons.

TABLE I. Systems and centrality classes used in this analysis. Listed for $p+p$, C+C, Si+Si, and six centralities of Pb+Pb collisions at 158A GeV are the number of events, the cross section of selected central interactions as percentage of the total inelastic cross section, and the mean number $\langle N_W\rangle$ of wounded nucleons.

Interaction	Number of events	$\sigma_{\text{cent.}}/\sigma_{\text{inel.}}$ (%)	$\langle N_W\rangle$
$p+p$	200K		
C+C	45K	15.3	14
Si+Si	65K	12.2	37
Pb+Pb (6)	38K	>43.5	45 ± 4
Pb+Pb (5)	20K	33.5–43.5	85 ± 7
Pb+Pb (4)	24K	23.5–33.5	128 ± 8
Pb+Pb (3)	24K	12.5–23.5	196 ± 6
Pb+Pb (2)	50K	5–12.5	281 ± 4
Pb+Pb (1)	38K	0–5	352 ± 3

III. DATA ANALYSIS

A. Data sets

The data sets used in the rapidity dependence study come from $p+p$, C+C, Si+Si, and Pb+Pb collisions at 158A GeV (Table I) and at 40A GeV (Table II). For Pb+Pb interactions, data with both central and minimum bias triggers were analyzed to study the centrality dependence of the BF. The minimum bias data were subdivided into six different

TABLE II. Systems and centrality classes used in this analysis. Listed for C+C, Si+Si, and six centralities of Pb+Pb collisions at 40A GeV are the number of events, the cross section of selected central interactions as percentage of the total inelastic cross section, and the mean number $\langle N_W\rangle$ of wounded nucleons.

Interaction	Number of events	$\sigma_{\text{cent.}}/\sigma_{\text{inel.}}$ (%)	$\langle N_W\rangle$
C+C	76K	65.7	9
Si+Si	43K	29.2	32
Pb+Pb (6)	45K	>43.5	43 ± 4
Pb+Pb (5)	27K	33.5–43.5	93 ± 7
Pb+Pb (4)	30K	23.5–33.5	142 ± 8
Pb+Pb (3)	32K	12.5–23.5	210 ± 6
Pb+Pb (2)	106K	5–12.5	290 ± 4
Pb+Pb (1)	190K	0–5	351 ± 3

TABLE III. The different energies for Pb+Pb interactions used to perform the energy scan. The cms energy of the system as well as the different beam energies, the cross section of selected central interactions as percentage of the total inelastic cross section, and the number of wounded nucleons are listed. The third number in the last column refers to the statistical error whereas the second refers to the systematic error.

$\sqrt{s_{NN}}$ (GeV)	E_{beam} (A GeV)	$\sigma_{\text{cent.}}/\sigma_{\text{inel.}}$ (%)	$\langle N_W \rangle$
6.3	20	7	$349 \pm 1 \pm 5$
7.6	30	7	$349 \pm 1 \pm 5$
8.8	40	5	$361 \pm 1 \pm 5$
12.3	80	7	$349 \pm 1 \pm 5$
17.3	158	5	362 ± 8

centrality classes [8] according to the energy recorded by the VCAL, from class Veto 1 (the most central collisions) to class Veto 6 (the most peripheral collisions) (Tables I and II). For the energy dependence study, we analyzed central Pb+Pb collisions throughout the whole SPS energy range (Table III). The most central Pb+Pb interactions for the highest SPS energy correspond to 5%, whereas for lower energies to 7.2% of the total geometric cross section.

B. Event and track selection

To reduce the contamination from non-target events and non-vertex tracks, selection criteria were imposed both at the event and at the track level.

Events were selected that had a proper position of the reconstructed primary vertex. The vertex coordinate V_z along the beam axis had to fulfill $|V_z - V_{z_0}| < \Delta z$, where the values of the central position V_{z_0} and the range Δz vary with respect to the system and the energy analyzed. In addition the vertex coordinates V_x and V_y perpendicular to the beam axis had to fulfill $|V_x - V_{x_0}| < \Delta x$ and $|V_y - V_{y_0}| < \Delta y$, where the values V_{x_0}, V_{y_0} and Δx, Δy also vary accordingly.

Selection criteria at the track level were imposed to reduce the contamination by tracks from weak decays, secondary interactions, and other sources of non-vertex tracks. Thus, an accepted track had to have an extrapolated distance of closest approach d_x and d_y of the particle at the vertex plane within the range $|d_x| < 2.0$ cm and $|d_y| < 1.0$ cm. In addition the potential number of points in the detector for the selected tracks had to be more than 30. To suppress double counting due to track splitting the ratio of the number of reconstructed points to the potential number of points was required to be larger than 0.5.

Finally, the NA49 detectors provide large acceptance in momentum space; however, the acceptance in the azimuthal angle ϕ is not complete. To avoid edge effects and to facilitate comparisons with model calculations, particles were selected in a restricted acceptance region [9]. The boundary of this region is described by

$$p_T(\phi) = \frac{1}{A + \left(\frac{D+\phi}{C}\right)^6} + B, \tag{3}$$

where the values of the parameters A, B, C, and D depend on the rapidity interval and on the energy and can be found in Ref. [9]. This restricted acceptance region is also imposed in the model calculations.

The fact that the azimuthal acceptance is not complete affects the results of our study. In particular, a percentage of the tracks that are excluded by the limited acceptance and by the acceptance filter from our analysis can be part of a pair of particles that are correlated in phase-space. If we also consider the fact that the width of the BF can be thought of as a measure of the number of correlated particles, then it is obvious that this effect tends to dilute our observable in a way that the value of the width increases. This is an essential point to take into account when comparing BF results between different experiments. Based on the previous, one can understand the importance of an apparatus with full ϕ acceptance (such as the STAR detectors or the future ALICE detector setup [10]) for studying the BF.

IV. RAPIDITY DEPENDENCE

To investigate the properties of hadronization in heavy ion collisions, as proposed by the BF methodology [1], we studied the system size and centrality dependence of the width of the BF at two SPS energies (158A and 40A GeV, corresponding to $\sqrt{s_{NN}} = 17.3$ and 8.8 GeV, respectively) and in two different pseudorapidity intervals. The selected pseudorapidity regions for $\sqrt{s} = 17.3$ GeV are $2.5 \leqslant \eta \leqslant 3.9$, named midrapidity region, and $4.0 \leqslant \eta \leqslant 5.4$, named forward rapidity region. The corresponding pseudorapidity regions for $\sqrt{s} = 8.8$ GeV are $1.8 \leqslant \eta \leqslant 3.2$ (midrapidity region) and $3.3 \leqslant \eta \leqslant 4.7$ (forward rapidity region). Figure 1 shows the resulting BF distributions for the two different energies (top and bottom panels, respectively) as a function of the pseudorapidity difference $\Delta\eta$ for central (left panel) and peripheral (right panel) Pb+Pb collisions.

The top panels of Fig. 2 show the width of the BF distributions for experimental data as a function of the mean number of wounded nucleons, for the two pseudorapidity regions (midrapidity region, left panel; forward rapidity region, right panel) for the $\sqrt{s_{NN}} = 17.3$ GeV case. The figure indicates that there is a clear centrality dependence for real data in the midrapidity region while this dependence vanishes in the forward region. To further investigate this effect, the Ultra-relativistic Quantum Molecular Dynamics model (UrQMD) [11], which is a microscopic model of (ultra)relativistic heavy ion collisions in the energy range from Bevalac and GSI Schwerionen Synchrotron (SIS) up to BNL Alternating Gradient Synchrotron (AGS), SPS, and RHIC, was used. The results from the study of this hadronic model as well as the widths obtained from shuffled[1] data [4,5] are also plotted in Fig. 2. No system size and centrality dependence, regardless of the rapidity region, is seen for either UrQMD or shuffled

[1]In shuffled events the particle (pseudo)rapidities in the event are randomly reassigned while the particle charges are unchanged. This procedure destroys (pseudo)rapidity correlations but retains global charge conservation effects.

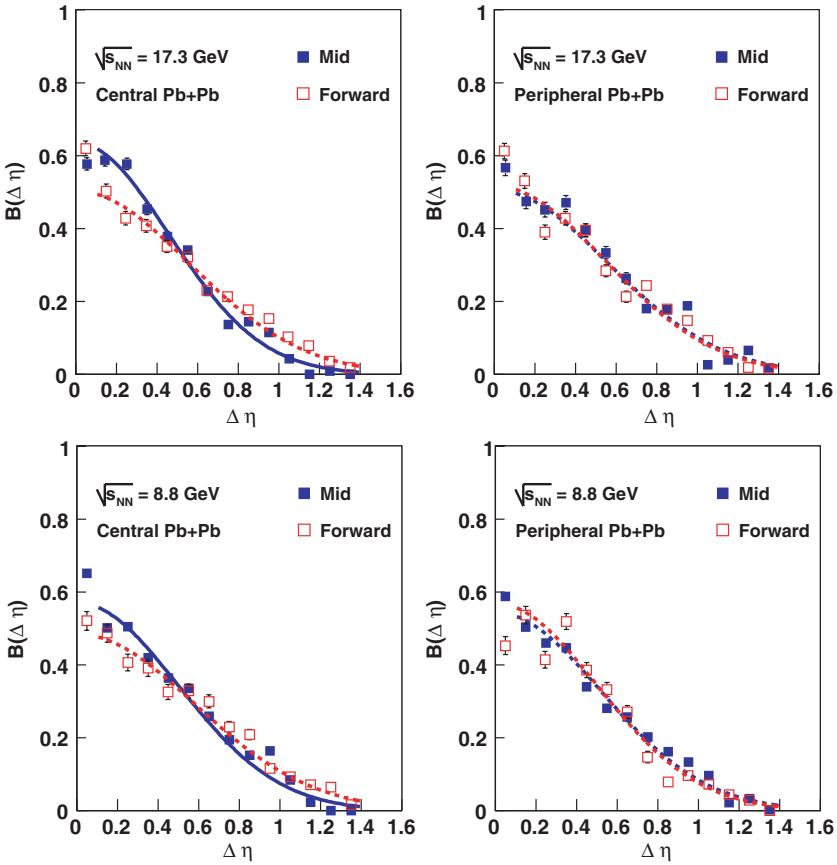

FIG. 1. (Color online) The BF as a function of the pseudorapidity difference $\Delta\eta$ for central (centrality class 1 of Tables I and II; left panels of this figure) and peripheral (centrality class 6 of Tables I and II; right panels of this figure) Pb+Pb collisions at $\sqrt{s_{NN}} = 17.3$ GeV (top panels) and $\sqrt{s_{NN}} = 8.8$ GeV (bottom panels) for the two rapidity regions. The curves drawn are Gaussian fits used to guide the eye.

events. The same behavior is observed for $\sqrt{s_{NN}} = 8.8$ GeV in the bottom panels of Fig. 2.

One should also note that there is no significant difference in the actual values of the widths between the two rapidity regions at both energies for the small systems, such as $p+p$ up to Si+Si. In other words, the difference in the absolute values appears only for the most central Pb+Pb collisions at both energies.

V. ENERGY DEPENDENCE

The energy dependence of the BF was studied for central Pb+Pb collisions for which NA49 data are available throughout the SPS energy range (100K events were analyzed for each energy). These data samples passed once again through the shuffling mechanism to provide an estimate of the highest value of the width for each energy under the constraint of global charge conservation. The pseudorapidity interval analyzed was limited to a range of 1.4 units and was located around midrapidity (Table IV). To compare the decrease of the width for the different energies, we introduced the normalized parameter W, which is defined by the following equation:

$$W = \frac{100 \cdot (\langle \Delta\eta \rangle_{\text{shuffled}} - \langle \Delta\eta \rangle_{\text{data}})}{\langle \Delta\eta \rangle_{\text{shuffled}}}. \qquad (4)$$

By using the measure W, we try to quantify the change of the BF width due to effects other than those of global charge conservation. Moreover, the slight changes of acceptance with energy should approximately cancel. Figure 3 shows as solid squares the BF distributions as a function of the pseudorapidity difference $\Delta\eta$ for central Pb+Pb collisions at $\sqrt{s_{NN}} = 12.3$ GeV (left panel), $\sqrt{s_{NN}} = 7.6$ GeV (middle panel), and $\sqrt{s_{NN}} = 6.3$ GeV (right panel). Figure 1 shows the results for the other two energies $\sqrt{s_{NN}} = 17.3$ GeV and $\sqrt{s_{NN}} = 8.8$ GeV.

The left panel of Fig. 4 shows the dependence of the normalized W parameter on $\sqrt{s_{NN}}$. For the data (red squares in Fig. 4), we note an indication for an increase with energy. In contrast, the results from the analysis of UrQMD generated events (blue boxes in Fig. 4) show no significant energy dependence of the measure W.

The right plot of Fig. 4 shows the dependence of the normalized W parameter on $\sqrt{s_{NN}}$ for the energy range of SPS together with the RHIC result at $\sqrt{s_{NN}} = 130$ GeV [5].

TABLE IV. Definition of the midrapidity as well as the forward rapidity interval for the different SPS energies.

$\sqrt{s_{NN}}$ (GeV)	η interval (midrapidity)	η (forward rapidity)
6.3	$1.6 \leqslant \eta \leqslant 3.0$	$3.1 \leqslant \eta \leqslant 4.5$
7.6	$1.7 \leqslant \eta \leqslant 3.1$	$3.2 \leqslant \eta \leqslant 4.6$
8.8	$1.8 \leqslant \eta \leqslant 3.2$	$3.3 \leqslant \eta \leqslant 4.7$
12.3	$2.2 \leqslant \eta \leqslant 3.6$	$3.7 \leqslant \eta \leqslant 5.1$
17.3	$2.5 \leqslant \eta \leqslant 3.9$	$4.0 \leqslant \eta \leqslant 5.4$

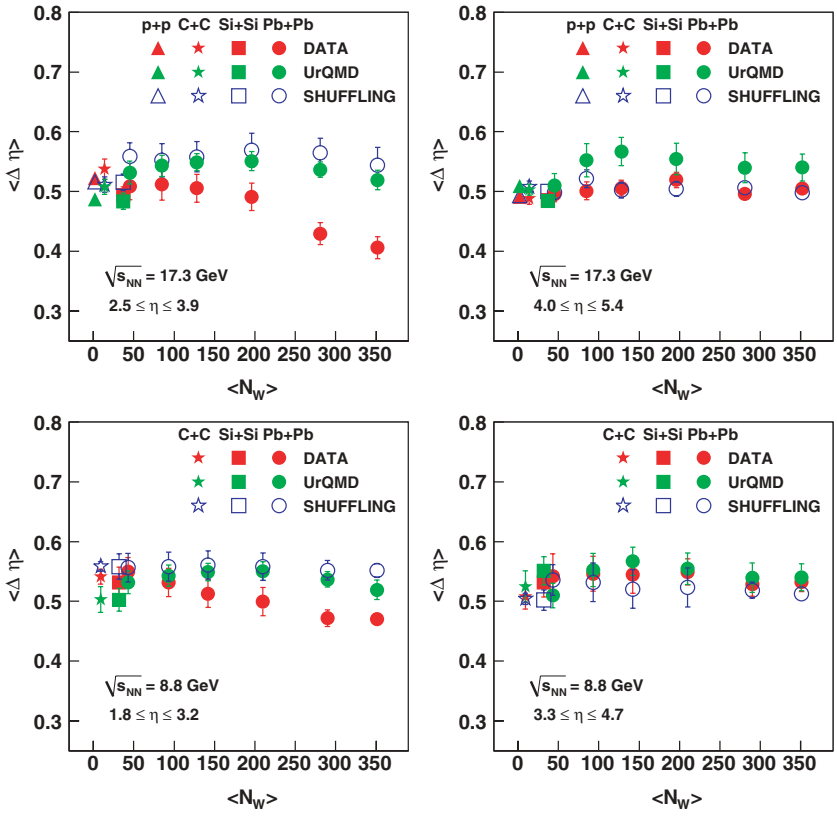

FIG. 2. (Color online) The system size and centrality dependence of the measured width $\langle\Delta\eta\rangle$ of the BF for charged particles at $\sqrt{s_{NN}} = 17.3$ GeV (top panels) and $\sqrt{s_{NN}} = 8.8$ GeV (bottom panels) plotted as a function of the mean number of wounded nucleons $\langle N_W\rangle$ for the midrapidity (left panels) and the forward rapidity (right panels) regions (see Table IV).

The corresponding RHIC point tends to be even higher than the last SPS one, indicating a continued rise of the W parameter toward RHIC and leaving an open question for the CERN Large Hadron Collider (LHC) energies.

Finally, we study the energy dependence of the scaled parameter W of the BF's width in the forward rapidity region (Table IV). The corresponding BF distributions for central Pb+Pb collisions are shown as open squares in Fig. 3 at $\sqrt{s_{NN}} = 12.3$ GeV (left panel), $\sqrt{s_{NN}} = 7.6$ GeV (middle panel), $\sqrt{s_{NN}} = 6.3$ GeV (right panel) and in Fig. 1 at $\sqrt{s_{NN}} = 8.8$ GeV (bottom left) and $\sqrt{s_{NN}} = 17.3$ GeV (top left). Figure 5 summarizes the main result from this study: The normalized parameter W shows no sign of an energy dependence in the forward rapidity regions.

VI. MODEL COMPARISON

In an attempt to interpret the results obtained for the centrality dependence of the BF width, several microscopic

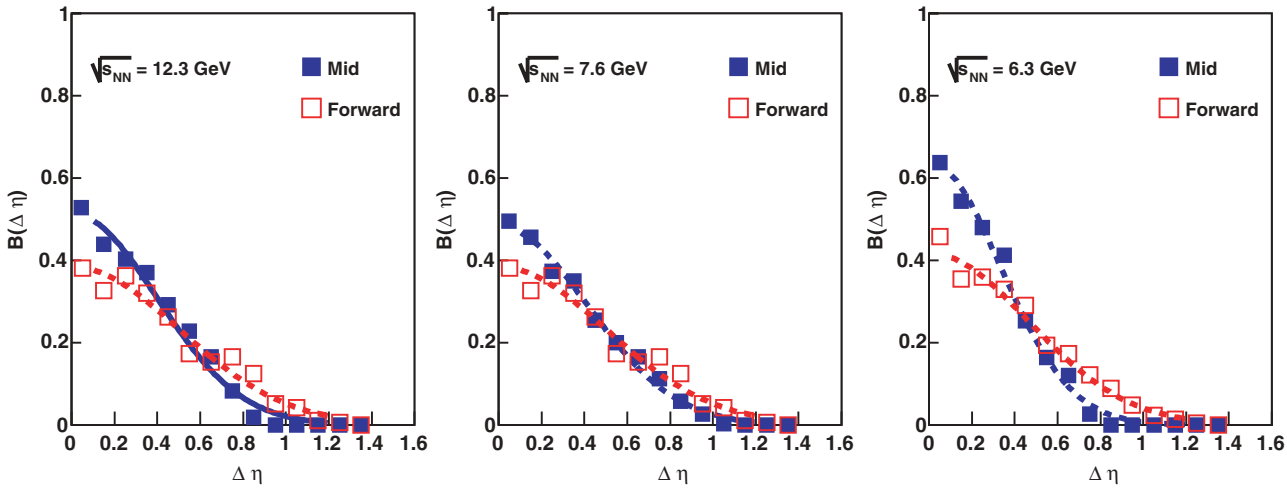

FIG. 3. (Color online) The BF as a function of the pseudorapidity difference $\Delta\eta$ for central Pb+Pb collisions at $\sqrt{s_{NN}} = 12.3$ GeV (left panel), $\sqrt{s_{NN}} = 7.6$ GeV (middle panel), and $\sqrt{s_{NN}} = 6.3$ GeV (right panel) for two rapidity regions (see Table IV). The curves drawn are Gaussian fits used to guide the eye.

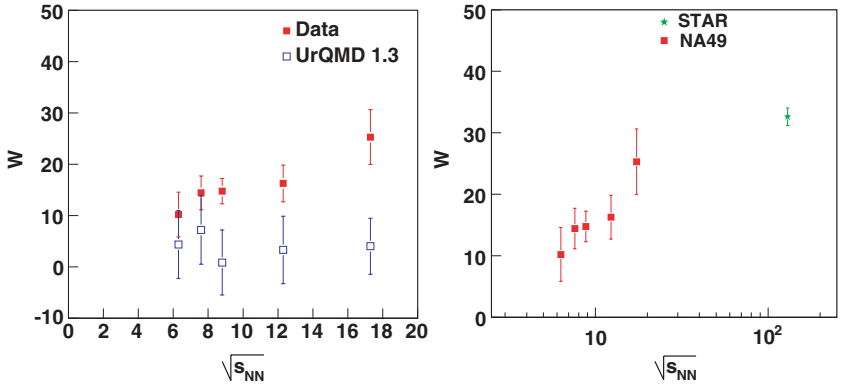

FIG. 4. (Color online) The dependence of the normalized parameter W on $\sqrt{s_{NN}}$ for central Pb+Pb collisions in the SPS energy range after applying the NA49 acceptance filter in comparison with the UrQMD results (left panel) and together with data for central Au+Au collisions at RHIC (right panel).

models were analyzed such as Heavy Ion Jet INteraction Generator (HIJING) [12], Ultra-relativistic Quantum Molecular Dynamics (UrQMD) [11], and A MultiPhase Transport model (AMPT) [13]. The first is based on the excitation of strings and their subsequent hadronization according to the LUND model [14]. The second is also based on string excitation with the addition of interactions between the produced particles after the hadronization (rescattering). The last is a multiphase transport model that contains a quark-parton transport phase before hadronization. In AMPT, the initial spatial and momentum distributions of partons and string excitations are obtained from HIJING. The parton cascade follows the ZPC model [15]. When the interactions of the partons cease, they are recombined with their parent strings to form hadrons according to the LUND fragmentation mechanism [14]. Then the scatterings of the produced hadrons are described by the ART model [16].

Figure 6, in which the measured width $\langle \Delta\eta \rangle$ of the BF for charged particles at $\sqrt{s_{NN}} = 17.3$ GeV is plotted as a function of the mean number of wounded nucleons $\langle N_W \rangle$, shows the main results of our comparison. The clear centrality dependence of the order of $17 \pm 3\%$ seen for experimental data cannot be described by the microscopic models HIJING and UrQMD. Results from both models suggest no centrality dependence of the BF width. On the other hand, the AMPT model, which incorporates the time evolution of partons before their hadronization, is predicting a centrality dependence of the BF similar to what is seen in the data.

More comprehensive model comparisons are in progress and will be addressed in a future publication.

VII. SUMMARY

In this article, we presented new results on the BF obtained by the NA49 collaboration. We analyzed data from different colliding systems and centrality classes for two different energies in two different rapidity regions. At midrapidity the experimental data reveal an interesting decrease of the BF width with increasing centrality of the collision for both energies. This effect cannot be reproduced either by the UrQMD model or by the shuffling mechanism. In the forward rapidity region, on the other hand, no centrality dependence of the BF width is observed.

The results from the energy scan show an indication for an energy dependence that is not apparent in the UrQMD model. The narrowing of the BF, expressed by the normalized width parameter W, increases from the lowest SPS energy to the highest SPS and RHIC energies. Again this rise is limited to the midrapidity regions.

Finally, the comparison with different microscopic models showed that the narrowing of the BF's width with centrality can

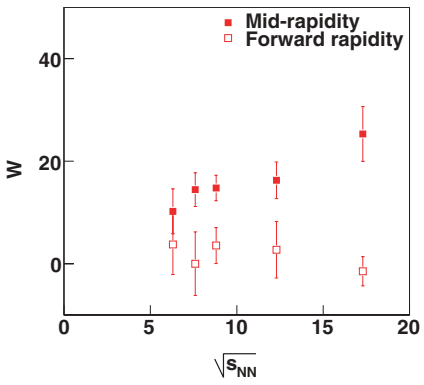

FIG. 5. (Color online) The dependence of the normalized parameter W on $\sqrt{s_{NN}}$ for central Pb+Pb collisions in the SPS energy range after applying the NA49 acceptance filter for the midrapidity and for the forward rapidity region (the intervals analyzed are given in Table IV).

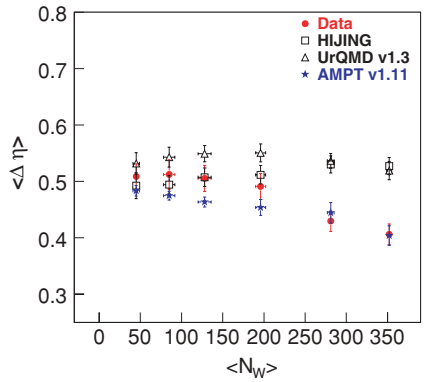

FIG. 6. (Color online) The centrality dependence of the measured width $\langle \Delta\eta \rangle$ of the BF at midrapidity ($2.5 \leqslant \eta \leqslant 3.9$) for charged particles produced in Pb+Pb collisions at $\sqrt{s_{NN}} = 17.3$ GeV as a function of the mean number of wounded nucleons $\langle N_W \rangle$. The plot shows the experimental data along with the predictions from different microscopic models.

only be reproduced by the model that contains a quark-parton evolution phase before hadronization. The latter might be a first indication that indeed the BF is related to the time of hadronization.

ACKNOWLEDGMENTS

This work was supported by the University of Athens project PYTHAGORAS II-Support of Univ. Research Groups; U.S. Department of Energy Grant DE-FG03-97ER41020/A000; the Bundesministerium fur Bildung und Forschung, Germany; the Virtual Institute VI-146 of Helmholtz Gemeinschaft, Germany; the Polish State Committee for Scientific Research (1 P03B 006 30, 1 P03B 097 29, 1 PO3B 121 29, and 1 P03B 127 30); the Hungarian Scientific Research Foundation (T032648, T032293, and T043514); the Hungarian National Science Foundation; OTKA (F034707); the Polish-German Foundation; the Korea Science & Engineering Foundation (R01-2005-000-10334-0); the Bulgarian National Science Fund (Ph-09/05); and the Croatian Ministry of Science, Education and Sport (Project 098-0982887-2878).

[1] S. A. Bass, P. Danielewicz, and S. Pratt, Phys. Rev. Lett. **85**, 2689 (2000).
[2] D. Drijard *et al*., Nucl. Phys. **B155**, 269 (1979); **B166**, 233 (1980).
[3] R. Brandelik *et al*., Phys. Lett. **B100**, 357 (1981); M. Althoff *et al*., Z. Phys. C **17**, 5 (1983); H. Aihara *et al*., Phys. Rev. Lett. **53**, 2199 (1984); H. Aihara *et al*., Phys. Rev. Lett. **57**, 3140 (1986); P. D. Acton *et al*., Phys. Lett. **B305**, 415 (1993).
[4] C. Alt *et al*. (NA49 Collaboration), Phys. Rev. C **71**, 034903 (2005); P. Christakoglou *et al*. (NA49 Collaboration), Nucl. Phys. **A749**, 279 (2005); AIP Conf. Proc. **828**, 107 (2006).
[5] J. Adams *et al*. (STAR Collaboration), Phys. Rev. Lett. **90**, 172301 (2003).
[6] S. Afanasiev *et al*. (NA49 Collaboration), Phys. Rev. C **66**, 054902 (2002); M. Gazdzicki (NA49 Collaboration), J. Phys. G **30**, S701 (2004).
[7] S. Afanasiev *et al*. (NA49 Collaboration), Nucl. Instrum. Methods A **430**, 210 (1999).
[8] G. Cooper, Ph.D. thesis, Department of Physics, University of California, Berkeley, 2000, LBNL-45467.
[9] J. Zaranek, Phys. Rev. C **66**, 024905 (2002); Diploma thesis, University of Frankfurt, 2003.
[10] ALICE Collaboration, J. Phys. G **30**, 1515 (2004); J. Phys. G **32**, 1295 (2006).
[11] M. Bleicher *et al*., J. Phys. G **25**, 1859 (1999).
[12] M. Gyulassy and X. N. Wang, Comput. Phys. Commun. **83**, 307 (1994).
[13] Z. W. Lin, C. M. Ko, B. A. Li, B. Zhang, and S. Pal, Phys. Rev. C **72**, 064901 (2005).
[14] T. Sjostrand, Comput. Phys. Commun. **82**, 74 (1994).
[15] B. Zhang, Comput. Phys. Commun. **109**, 307 (1998).
[16] B. A. Li and C. M. Ko, Phys. Rev. C **52**, 2037 (1995).